Cite this article
Feng S and Vardanega PJ (2019)
Correlation of the hydraulic conductivity of fine-grained soils with water content ratio using a database.
Environmental Geotechnics **6(5)**: 253–268,
https://doi.org/10.1680/jenge.18.00166

Research Article
Paper 1800166
Received 24/10/2018; Accepted 05/06/2019
Published online 31/07/2019

Keywords: geotechnical engineering/porous-media characterisation/statistical analysis

Environmental Geotechnics

ice Publishing

Correlation of the hydraulic conductivity of fine-grained soils with water content ratio using a database

Shuyin Feng MSc (Bristol)
PhD student, Department of Civil Engineering, University of Bristol, Bristol, UK
(Orcid:0000-0002-3837-6762)

Paul J. Vardanega PhD (Cantab), GMICE, MASCE, MIEAust, FHEA
Senior Lecturer in Civil Engineering, Department of Civil Engineering, University of Bristol, Bristol, UK (corresponding author: p.j.vardanega@bristol.ac.uk) (Orcid:000-0001-7177-7851)

The saturated hydraulic conductivity of fine-grained soils is of great importance, as it is directly linked to many fundamental calculations in geotechnical engineering. In this paper, various models for predicting saturated hydraulic conductivity using simple soil parameters are reviewed. A simplified semi-empirical prediction equation using water content ratio (w/w_L) as the predictor of saturated hydraulic conductivity is calibrated using a large database called FG/KSAT-1358 (n > 1300) of saturated hydraulic conductivity (k_{sat}) measurements on fine-grained materials. The regression equation can predict the saturated hydraulic conductivity of the measurements included in the database to within plus or minus an order of magnitude around 90% of the time. To study other factors which may affect the values of k_{sat}, the database is then subdivided according to liquid limit level, silt or clay classification, hydraulic conductivity test method and sample condition. Some variations in the regression equations for each of the aforementioned subsets are observed, but the effect on the value of the exponent in the derived power-law relationships is relatively minor.

Notation

a	regression constant
b	regression constant
C	constant
D_R	specific weight of the solid
d	particle size
e	void ratio
e_L	void ratio at the liquid limit
G_S	specific gravity
$\boldsymbol{g}$	gravitational acceleration (length/time^2)
I_P	plasticity index (%)
k	hydraulic conductivity (length/time)
k_{sat}	saturated hydraulic conductivity (length/time)
L	length
n	number of data points
RD	relative deviation [RD = $100(1–R^2)^{1/2}$]
R^2	coefficient of determination
S_S	specific surface area (length^2/mass)
T	time
w	water content (%)
w_L	liquid limit (%)
w_P	plastic limit (%)
w_S	shrinkage limit (%)
z	regression model parameter
α	regression constant
β	exponent
δ	coefficient
μ	coefficient
μ_w	dynamic viscosity of the permeant (mass/(time × length))
ν	exponent
ρ_w	density of the permeant (mass/length^3)

Introduction

Reliable a priori assessments of the saturated hydraulic conductivity (k_{sat}) of fine-grained soils are useful for geotechnical and geoenvironmental engineers. The saturated hydraulic conductivity is directly linked to the seepage and consolidation characteristics of clays and silts (Chapuis, 2012; Leroueil *et al.*, 1990; Pane *et al.*, 1983; Tavenas *et al.*, 1983a, 1983b). Fine-grained soils are often used in the construction of geostructures such as waste-disposal facilities (Bannour *et al.*, 2016; Benson and Trast, 1995; O'Kelly, 2016; Terzaghi *et al.*, 1996), road slopes and embankments (Walker and Raymond, 1968) and earth dams (Terzaghi *et al.*, 1996), and the need to model the flow of water through such structures is required for assessing serviceability and stability. For landfill applications, the k_{sat} of the clay liner is often the 'governing parameter' (e.g. Amadi and Alih, 2019). Saturated hydraulic conductivity is also important in the assessment of slope stability (e.g. Hamm *et al.*, 2006).

This paper presents a simple prediction model for saturated hydraulic conductivity calibrated with a large database (n > 1300) of laboratory tests (FG/KSAT-1358) on a wide variety of fine-grained soils. The use of geodatabases to develop 'transformation models' for a priori estimation of soil parameters is valuable in geotechnical and geoenvironmental engineering (cf. Ching *et al.*, 2017; Kulhawy and Mayne, 1990; Phoon and Kulhawy, 1999a, 1999b). It should be noted that to predict the hydraulic conductivity of 'unsaturated' fine-grained materials, alternative approaches are needed (see e.g. the publications by Mualem (1976), Olson and Daniel (1981), Santoso *et al.* (2011) and Dong *et al.* (2018)). Also, composite soils (including sands) (e.g. Al-Moadhen *et al.*, 2018) and modified soils (e.g. Azad *et al.*, 2015) are beyond the scope of this work, and such data are not included in the database presented in this paper.

Literature review

Chapuis (2012) comprehensively reviewed various empirical and semi-empirical approaches to predicting the hydraulic conductivity of soils. The 'Kozeny–Carman' equation (Carman, 1937, 1939; Kozeny, 1927) is a commonly used semi-empirical approach which relates the hydraulic conductivity k (length (L)/time (T)) to the specific surface (S_S) and the void ratio function $e^3/(1+e)$. Equation 1 is the form of the Kozeny–Carman equation shown in the paper by Chapuis and Aubertin (2003)

$$k = C\frac{\boldsymbol{g}}{\mu_w \rho_w}\frac{e^3}{S_S^2 D_R^2(1+e)} \tag{1}$$

where C is a constant; $\boldsymbol{g}$ is the gravitational acceleration; μ_w is the dynamic viscosity of the permeant; ρ_w is the density of the permeant (e.g. water); e is the void ratio; and D_R is the specific weight of the solid material. Variants of Equation 1 have been used to predict the saturated hydraulic conductivity of soils (e.g. Chapuis and Aubertin, 2003; Mbonimpa *et al*., 2002; Ren and Santamarina, 2018; Ren *et al*., 2016; Sanzeni *et al*., 2013).

Carrier and Beckman (1984) indicated that for remoulded clays the hydraulic conductivity can be correlated with w_P, I_P and e, by way of

$$k_{sat}(\mathrm{m/s}) = \mu\frac{(e-\delta)^{\nu}}{1+e} \tag{2}$$

where $\mu = (0{\cdot}389/w_P)^{4{\cdot}29}$; $\delta = 0{\cdot}027(w_P - 0{\cdot}242 I_P)$; $\nu = 4{\cdot}29$; w_P is the plasticity limit; and I_P is the plasticity index. Equation 2 requires a variable exponent on the void ratio (e).

Specific surface

Sanzeni *et al*. (2013) explained that the success of the use of variants of Equation 1 for the prediction of k_{sat} relies on a good estimate or proxy for specific surface being available. Past studies (e.g. Farrar and Coleman, 1967; Muhunthan, 1991; Sridharan *et al*., 1988) showed that specific surface S_S and liquid limits w_L are correlated for a variety of plastic soils. Chapuis and Aubertin (2003) derived a linear relationship between $1/S_S$ and $1/w_L$ (Equation 3) for different types of clays using a database gathered from five publications (De Bruyn *et al*., 1957; Farrar and Coleman, 1967; Locat *et al*., 1984; Sridharan *et al*., 1986a, 1988)

$$\frac{1}{S_S(\mathrm{m^2/g})} = 1{\cdot}3513\left(\frac{1}{w_L}\right) - 0{\cdot}0089 \tag{3}$$

Chapuis (2012) suggested that by replacing S_S with w_L in the Kozeny–Carman equation, the saturated hydraulic conductivity k_{sat} may be correlated with $e^3/[w_L^2(1+e)]$. Chapuis (2012) developed a correlation based on data from Quebec Champlain Sea Clay

$$k_{sat} = 6{\cdot}68\times10^{-6}\left[\frac{e^3}{(1+e)(w_L^{-1}+z)^2}\right]^{1{\cdot}339}$$

$$R^2 = 0{\cdot}81 \tag{4}$$

where $z = 0{\cdot}00836$ is determined by the least-squares method using experimental data for the specific clay studied – that is, Quebec Champlain Sea Clay.

By using w_L (for fine-grained soils) and cumulative grain size distribution (for sandy soils) to estimate S_S, Ren and Santamarina (2018) developed a hydraulic conductivity prediction model (Equation 5) for a wide range of sediments calibrated using a laboratory database

$$\frac{k}{\mathrm{cm/s}} = 10^{-5}\left(\frac{S_S}{\mathrm{m^2/g}}\right)^{-2} e^{\beta} \tag{5}$$

As reported by Ren and Santamarina (2018), the values predicted using Equation 5 mostly fall within the $k_{measured}/5 \leq k_{predict} \leq 5k_{measured}$ range based on their database. Ren and Santamarina (2018) used a correlation between S_S and w_L to derive missing values of S_S in their database. It is worth noting that significant scatter below $k_{measured} < 10^{-5}$ cm/s (the clay/silt material region) can be observed on the predicted-against-measured plot – wider than the general range $k_{measured}/5 \leq k_{predict} \leq 5k_{measured}$ quoted. This paper focuses on clay and silt soils with k_{sat} generally less than 10^{-5} cm/s.

Shrinkage limit

Sridharan and Nagaraj (2005) found that the shrinkage limit (w_S) is also important for the prediction of the hydraulic conductivity, as well as the w_L, of remoulded fine-grained soils when developing the following equation

$$k = \alpha\left[\frac{e^x}{1+e}\right] \tag{6}$$

where $x = 4$ based on the regression analysis and $C = 2{\cdot}5\times10^{-4}(w_L - w_S)^{-3{\cdot}69}$. However, despite being a key soil mechanics parameter (e.g. Hobbs *et al*., 2018), w_S is not as often measured as w_L during routine field and laboratory investigations and therefore could not be used in the analysis in this paper (it was rarely reported in the examined publications).

Void ratio function

Various studies have used a simple power-law correlation (e.g. Equation 7) for predicting the hydraulic conductivity of soils (e.g. Al-Tabbaa and Wood, 1987; Dolinar, 2009; Mesri and Olson, 1971a; Samarasinghe *et al*., 1982)

$$k = ae^b \tag{7}$$

where a and b are regression constants.

Vardanega *et al*. (2017), using a small database (n = 119) of falling and constant head hydraulic conductivity test results, showed that for the prediction of the hydraulic conductivity of a single type of clay, Equation 7 is statistically acceptable. Vardanega *et al*. (2017) showed that the exponent b varies from 1·53 to 5·32 for ten different types of soils.

Water content ratio

The e/e_L ratio (or the w/w_L ratio) is also used in many soil behaviour correlations – for example, in the paper by Nagaraj and Srinivasa Murthy (1986) for clay compressibility; in the paper by Griffiths and Joshi (1988) for clay cementation; and for modelling undrained shear strength variation of fine-grained soils (Kuriakose *et al*., 2017; Spagnoli and Feinendegen, 2017). Nagaraj *et al*. (1993, 1994) proposed Equations 8 (for normally consolidated materials) and 9 (for overconsolidated materials) to predict the hydraulic conductivity of fine-grained soils by introducing the void ratio at the liquid limit (e_L) as a normaliser of e. This approach is elegant, as e_L, which can be reduced to w_L (as shown previously), is a good predictor of the specific surface of fine-grained soils.

8. $$\frac{e}{e_L} = 2{\cdot}38 + 0{\cdot}233 \log k$$

9. $$\frac{e}{e_L} = 2{\cdot}162 + 0{\cdot}195 \log k$$

While not stated explicitly in the papers by Nagaraj *et al*. (1993, 1994) for Equations 8 and 9, as shown here k is in centimetres per second (as also stated in the papers by Sridharan and Nagaraj (2005) and Chapuis (2012)) when discussing Equation 8. Sivapullaiah *et al*. (2000) also used the e/e_L ratio when investigating various functions predicting the hydraulic conductivity of soils. Mbonimpa *et al*. (2002) also showed that e/e_L (w/w_L) correlated with k_{sat} based on a database (n = 342) (given here as Equation 10) using data from six publications (Al-Tabbaa and Wood, 1987; Leroueil *et al*., 1990; Nagaraj *et al*., 1994; Raymond, 1966; Sivapullaiah *et al*., 2000; Tan, 1989) with prediction bounds of approximately 0·2–5 times the measured value. This paper aims to calibrate an equation for k_{sat} using w/w_L and a much larger database. Equation 10 was generated partly using all the data in the paper by Sivapullaiah *et al*. (2000), which included tests on soil mixtures containing sand. In this paper, the data used are for soils classified as fine-grained.

10. $$k(\text{cm/s}) = 7 \times 10^{-8}\left(\frac{e}{e_L}\right)^{3{\cdot}15} \qquad n = 342$$

Database

The database comprises over 1300 experimental values of k_{sat} on over 130 different types of clay samples sourced from over 30 publications. The database includes the data sources examined in the paper by Vardanega *et al*. (2017) with the data from the paper by Chung *et al*. (2002) excluded due to the lack of relevant information on w_L. Table 1 summarises the key information relating to the sources used to generate the database. The following hydraulic conductivity test methods are represented in the database: constant-head test, falling-head test, flow-pump test and consolidation test. Hydraulic conductivity anisotropy is beyond the scope of this paper, and the hydraulic conductivity measurements aggregated in this database were all measured vertically. Only test results for saturated hydraulic conductivity k_{sat} measured with water as the permeant were included in the database. The database comprises tests conducted on both samples derived from natural soils and artificially fabricated 'laboratory soils'. As the natural soils generally contain some percentage of coarse material, soil mixtures with less than 50% coarse particles (d > 75 µm) and a measured plasticity limit have been classified as fine-grained materials and thus have been included in the database. For the laboratory soils, only tests on samples made from pure clay have been included.

Temperature effects

Due to the lack of available test temperature information from most sources (cf. Table 1), the collected k_{sat} could not be corrected to the intrinsic permeability K. Given that the k_{sat} measurements in the database were laboratory measurements, it was assumed that the test temperature (where not quoted) was not significantly different between different laboratories. It is acknowledged that some of the scatter in the correlations shown in this paper was possibly due to temperature effects.

Soil classification

The Atterberg limits of the collected data are plotted on a Casagrande chart in Figure 1 (chart design based on the standard by ASTM (2017)). Using the classification framework given in the standard by ASTM (2017), the database consists of 31% lean clays (w_L < 50, I_P > 7 and plots on or above the 'A' line, as shown in Figure 1), 5% silts (w_L < 50, I_P < 4 or plots below the A line), 38% fat clays ($w_L \geq$ 50, I_P plots on or above the A line) and 20% elastic silts ($w_L \geq$ 50, I_P plots below the A line). One sample was classified as clayey sand, and 75 samples were without I_P or Unified Soil Classification System (USCS) information and thus were left unclassified.

Analysis

Statistical measures

The coefficient of determination (R^2) is given for the correlations in this paper. For example, an R^2 of 0·50 suggests that it explains 50% of the variability of the data (see the book by Montgomery *et al*. (2007: p. 294)). When performing correlation analyses, computing only the coefficient of determination (R^2) does not allow for adequate justification of the strength of a correlation

Table 1. Summary of the database FG/KSAT 1358 (continued on next page)

Sources[a]	Materials	n	e range	k_{sat} range: m/s	k test method	Test T: °C	w_L	I_P	Atterberg limit test method[b]	Clay fraction (<2 μm): %	G_S	USCS[c]	Remarks
Raymond (1966)	Bentonite, Don Valley Clay, New Liskeard Clay, Leda Clay	123	0·51–2·30	$1{\cdot}49 \times 10^{-12}$–$3{\cdot}56 \times 10^{-9}$	Consolidation test, falling-head test	—	33·4–118	17·1–72·2	—	28–83	—	CL, CH	
Walker and Raymond (1968)[d]	Leda Clay	8	0·83–1·47	$8{\cdot}11 \times 10^{-11}$–$9{\cdot}16 \times 10^{-10}$	Falling-head test	—	36	13	—	57		CL	The Atterberg limits and clay fraction are rough estimates based on averaged values from previous studies
Mesri and Olson (1971b)	Calcium (Ca) montmorillonite	71	1·08–6·11	$1{\cdot}99 \times 10^{-13}$–$4{\cdot}39 \times 10^{-9}$	Consolidation test	—	189–220	157–187	ASTM	—	2·8	CH	
Mesri and Olson (1971a)	Kaolinite	19	0·87–2·24	$1{\cdot}49 \times 10^{-10}$–$2{\cdot}14 \times 10^{-8}$	Consolidation test	—	45	16	—	47	2·65	ML	see note f
Salem and Krizek (1973)	Dredging slurries	22	0·55–2·15	$1{\cdot}30 \times 10^{-11}$–$1{\cdot}42 \times 10^{-9}$	Consolidation test	—	61, 71	30, 44	—	30, 40		CH, MH	
Bartos (1977)	Dredged materials	5	0·87–1·12	4×10^{-11}–$2{\cdot}9 \times 10^{-10}$	Consolidation test	Usually 20	42–129	19–97	—	13–58		CH, CL, SC	
Chamberlain and Gow (1979)	CRREL clay, Morin Clay, Ellsworth Clay	63	0·65–1·87	$1{\cdot}96 \times 10^{-10}$–$4{\cdot}29 \times 10^{-6}$	Falling-head test	≈22	26–45	5–20	—	—	2·66–2·77	ML, CL	Including 29 frozen-and-thawed samples
Samarasinghe *et al.* (1982)	Greyish clay	12	0·32–0·57	$1{\cdot}75 \times 10^{-11}$–$4{\cdot}79 \times 10^{-10}$	Flow-pump test	—	27	14	—	—	—	CL	
Pane *et al.* (1983)	Kaolinite	37	1·00–3·55	$8{\cdot}23 \times 10^{-10}$–$2{\cdot}15 \times 10^{-7}$	Falling-head test, flow-pump test	—	53·6	21·7	—	—	2·66	MH	
Tavenas *et al.* (1983b)[d]	Natural soil	27	0·84–2·48	$3{\cdot}13 \times 10^{-10}$–$5{\cdot}11 \times 10^{-9}$	Constant-head test	21 ± 0·5	34–65	15–39	—	54·5–81		CH, CL	
Tavenas *et al.* (1983a)[d]	Louiseville Clay	5	1·27–2·19	$1{\cdot}67 \times 10^{-10}$–$1{\cdot}45 \times 10^{-9}$	Falling-head test	—	62	37	—	85	—	CH	
Sridharan *et al.* (1986b)	Bentonite	44	0·81–7·48	$8{\cdot}72 \times 10^{-13}$–$1{\cdot}73 \times 10^{-10}$	Consolidation test	20	108–675	47·5–625·9	Casagrande method	—	2·59–2·81	CH, MH	
Al-Tabbaa and Wood (1987)	Speswhite kaolin	33	0·96–2·21	$4{\cdot}55 \times 10^{-10}$–$6{\cdot}00 \times 10^{-9}$	Falling-head test	—	69	31	—	80		MH	
Tan (1989)	Silty marine clay, marine clay	13	1·08–2·25	$7{\cdot}84 \times 10^{-11}$–$1{\cdot}10 \times 10^{-9}$	Falling-head test	—	80, 108	54, 78	—	—	2·65, 2·7	CH	e adopted here is the averaged value
Chandler *et al.* (1990)[d]	London Clay	11	0·68–0·87	$5{\cdot}28 \times 10^{-12}$–$2{\cdot}3 \times 10^{-11}$	Constant-head test	20	85	59	BS 1377:1975 (BSI, 1975)	66	2·72	CH	
Leroueil *et al.* (1990)[d]	Louiseville Clay, St Esprit Clay, Backebol Clay, Matagami A, Matagami B	33	0·93–2·37	$8{\cdot}69 \times 10^{-11}$–$2{\cdot}51 \times 10^{-9}$	Constant-head test, falling-head test	—	41–88	19–56	—	55–80		CL, CH	
Towhata *et al.* (1993)	MC clay, bentonite	16	0·81–8·57	$1{\cdot}44 \times 10^{-13}$–$2{\cdot}09 \times 10^{-9}$	Consolidation test	20	70, 450	29, 421	—	—	2·75, 2·78	CH, MH	Including only test results at 20°C
Nagaraj *et al.* (1993)	Black cotton soil, brown soil, red soil, bentonite	23	0·57–7·048	$1{\cdot}15 \times 10^{-11}$–$1{\cdot}83 \times 10^{-9}$	Falling-head test	—	50–300	23–230	—	—	2·65, 2·8	MH, CH	—

Table 1. Continued

Sources[a]	Materials	*n*	e range	k_{sat} range: m/s	*k* test method	Test *T*: °C	w_L	I_P	Atterberg limit test method[b]	Clay fraction (<2 μm): %	G_S	USCS[c]	Remarks
Nagaraj *et al.* (1994)	Black cotton, soil, brown soil, red soil, marine soil	70	0·56–2·37	$9{\cdot}19 \times 10^{-12}$ $-1{\cdot}82 \times 10^{-9}$	Falling-head test	—	50–106	23–59	—	—	2·64–2·67	MH, CH	—
Benson and Trast (1995)	Mine spoil, loess, glacial till, marine sediment, alluvial, glacio-lacustrine	190	0·29–1·38	9×10^{-12} $-7{\cdot}5 \times 10^{-6}$	Falling-head test	—	24–70	11–46	ASTM D 4318 (version unspecified)	16–65	2·68–2·9	CL, CH	e is calculated based on the reported dry unit weight γ_d and specific gravity G_S
Siddique and Safiullah (1995)	Dhaka Clay	11	0·51–0·97	$7{\cdot}30 \times 10^{-11}$ $-9{\cdot}72 \times 10^{-10}$	Constant-head test, consolidation test		40	20	—	22	2·68	CL	
Dewhurst *et al.* (1996)	Marine clay	12	0·19–0·94	$2{\cdot}99 \times 10^{-12}$ $-1{\cdot}98 \times 10^{-10}$	Flow-pump test	—	58	32	—	—	2·68	CH	
Pane and Schiffman (1997)	Speswhite kaolin	8	1·29–4·13	$8{\cdot}98 \times 10^{-10}$ $-1{\cdot}05 \times 10^{-7}$	Flow-pump test	22 ± 0·5	53	21	—	75	2·6	MH	
Clennell *et al.* (1999)	Silty clay, Speswhite kaolin, calcium montmorillonite, natural clay	39	0·32–2·53	$4{\cdot}45 \times 10^{-13}$ $-4{\cdot}34 \times 10^{-9}$	Flow-pump test	—	55–120	31–34	—	—	2·61–2·69	CH, MH	
Sivapullaiah *et al.* (2000)	Bentonite, silt, silt-and-bentonite mixtures	102	0·61–5·98	$1{\cdot}27 \times 10^{-12}$ $-3{\cdot}46 \times 10^{-8}$	Consolidation test	—	35–344	—	Cone-penetration method	8–100	—	—	
Lekha *et al.* (2003)	Local IIT clay, calcium bentonite	12	0·48–1·84	$3{\cdot}20 \times 10^{-11}$ $-1{\cdot}23 \times 10^{-9}$	Falling-head test	—	47, 97	—	—	—		CL, MH	
Sridharan and Nagaraj (2005)	Red earth, silty soil, kaolinite, Cochin Clay, brown soil, illitic soil	63	0·53–1·84	$1{\cdot}20 \times 10^{-11}$ $-6{\cdot}89 \times 10^{-8}$	Falling-head test	20 ± 1	37–73·4	9·5–26·4	BS 1377:1990 (BSI, 1990) cone-penetrometer method	5–35	2·58–2·7	CL, ML, MH	
Shafiee (2008)	Illite, montmorillonite	6	0·28–0·59	$6{\cdot}60 \times 10^{-9}$ $-1{\cdot}07 \times 10^{-6}$	Constant-head test	22 ± 0·5	29·5, 69	20, 31	—	—	2·72, 2·74	CL, MH	Not included in the analysis of Equation 12 and after, as the data points are potentially outliers.
Dolinar (2009)	Crystallised kaolinite, calcium montmorillonite, kaolinite-and-calcium montmorillonite mixture	25	0·86–2·5	$1{\cdot}6 \times 10^{-10}$ $-4{\cdot}95 \times 10^{-9}$	Falling-head test	20	40·1–129	25·9–39·5	—	—	—	ML, MH	
Horpibulsuk *et al.* (2011)	Kaolin, bentonite, Bangkok Clay	79	0·63–3·58	$1{\cdot}30 \times 10^{-12}$ $-9{\cdot}22 \times 10^{-10}$	Consolidation test	23	54–131	28–105	Casagrande method	—	2·63–2·66	CH	
Adams *et al.* (2013)	Boston Blue Clay	11	0·58–0·97	$3{\cdot}57 \times 10^{-11}$ $-5{\cdot}52 \times 10^{-10}$	Constant-head test	26 ± 0·1	46	23	—	53	2·78	CL	
Kim *et al.* (2013)[d]	Marine sediments	43	0·59–1·95	$1{\cdot}31 \times 10^{-11}$ $-8{\cdot}52 \times 10^{-9}$	Consolidation test	—	38·8–77	11·2–28	ASTM D 4318 (version unspecified) Casagrande method	—	2·45–2·74	ML, MH	

Table 1. Continued

Sources[a]	Materials	n	e range	k_{sat} range: m/s	k test method	Test T: °C	w_L	I_P	Atterberg limit test method[b]	Clay fraction (<2 µm): %	G_S	USCS[c]	Remarks
Sanzeni *et al.* (2013)[e]	Fine-grained soil	122	0·33–1·21	$1{\cdot}2 \times 10^{-11}$ – $1{\cdot}52 \times 10^{-6}$	Constant-head test, consolidation test, falling-head test	—	22–71	5–46	ASTM D 4318-10 (ASTM, 2010)	—	—	CL, ML, CH, MH	
Total		1358	0·19–8·57	$1{\cdot}44 \times 10^{-13}$ – $7{\cdot}5 \times 10^{-6}$			22–675	5–625·9		5–85	2·09–2·9		

[a]Data by Walker and Raymond (1968), Pane *et al.* (1983), Al-Tabbaa and Wood (1987), Leroueil *et al.* (1990) and Lekha *et al.* (2003) were also used by Vardanega *et al.* (2017). Data by Mesri and Olson (1971a), Horpibulsuk *et al.* (2011), Raymond (1966), Siddique and Safiullah (1995), Tavenas *et al.* (1983a, 1983b), Dolinar (2009), Sanzeni *et al.* (2013), Kim *et al.* (2013), Sridharan and Nagaraj (2005) and Sivapullaiah *et al.* (2000) were also used in the database of Ren and Santamarina (2018). Data by Raymond (1966), Al-Tabbaa and Wood (1987), Tan (1989), Leroueil *et al.* (1990), Nagaraj *et al.* (1994) and Sivapullaiah *et al.* (2000) were also used by Mbonimpa *et al.* (2002). Note: hydraulic conductivity data without corresponding Atterberg limits were not included in this database, and hydraulic conductivity data of the flow-pump tests in the study by Pane *et al.* (1983) were also added in this study

[b]For the publications specified, some used the fall-cone test, while some used the Casagrande method in w_L measurement. O'Kelly *et al.* (2018) showed that the test values tend to be similar up to w_L equal to 120%; the Casagrande method tends to give higher test results when w_L > 120%

[c]CH, fat clay; CL, lean clay; MH, elastic silts; ML, silts; SC, clayey sand (abbreviations follow ASTM (2017))

[d]Provided test results on undisturbed samples

[e]The exact sample states are not specified

[f]Only the kaolinite data was included in the database range of liquid limit values reported was considered sufficiently narrow to justify using average values of the Atterberg limits in the analysis

CRREL, Cold Regions Research and Engineering Laboratory, USCS, Unified Soil Classification System

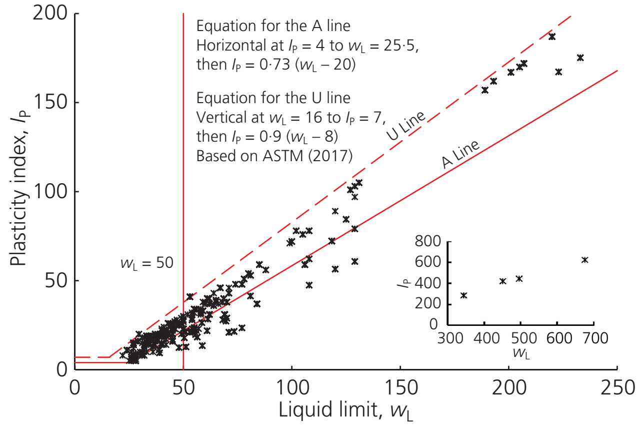

Figure 1. Database soils plotted on a Casagrande chart (73% clays and 27% silts) (chart design based on ASTM (2017))

(Kulhawy and Mayne, 1990). In the correlation analyses in this paper, the R^2, number of data points (n) and the standard error (SE) are quoted following the approach shown in the report by Kulhawy and Mayne (1990). Quoting the SE (sometimes referred to as the standard deviation) is important as it gives a measure of the 'transformation uncertainty' of the correlations (see the papers by Phoon and Kulhawy (1999a, 1999b)). In addition, the p-value of the correlation is quoted, which is the probability that one would say that no correlation exists (i.e. rejection of the null hypothesis), as well as the relative deviation (RD), which gives the percentage of error about the fitted line against a horizontal fit (average value) (see the paper by Waters and Vardanega (2009)).

Regression analyses

The available $1/S_S$ values from the database were plotted against $1/w_L$ in Figure 2, and Equation 11 was produced

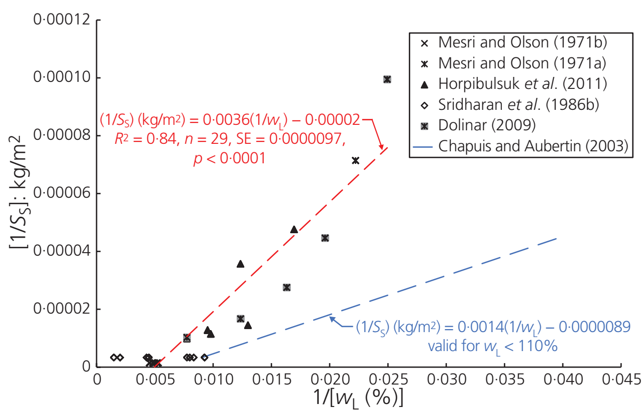

Figure 2. $1/S_S$ plotted against $1/w_L$ (Equation 3 also shown for comparison; S_S information for Sridharan *et al.* (1986b) is given in Sridharan and Choudhary (2008); note: the trend line from the paper by Chapuis and Aubertin (2003) is based on a separate soil database)

$$\frac{1}{S_S}\left(\frac{\text{kg}}{\text{m}^2}\right) = 0{\cdot}0036\left(\frac{1}{w_L}\right) - 0{\cdot}000018$$

$$(R^2 = 0{\cdot}84, \;\; n = 29, \;\; \text{SE} = 0{\cdot}0000097, \;\; p < 0{\cdot}0001)$$

11.

Equation 11, along with Equation 3, further confirms that w_L can be used as a substitute for S_S.

Figures 3(a) and 3(b) show that when considering the entire database (n > 1300), w_L and e are poor predictors of k_{sat}. However, Figure 3(b) shows visually that k_{sat} is related to e for

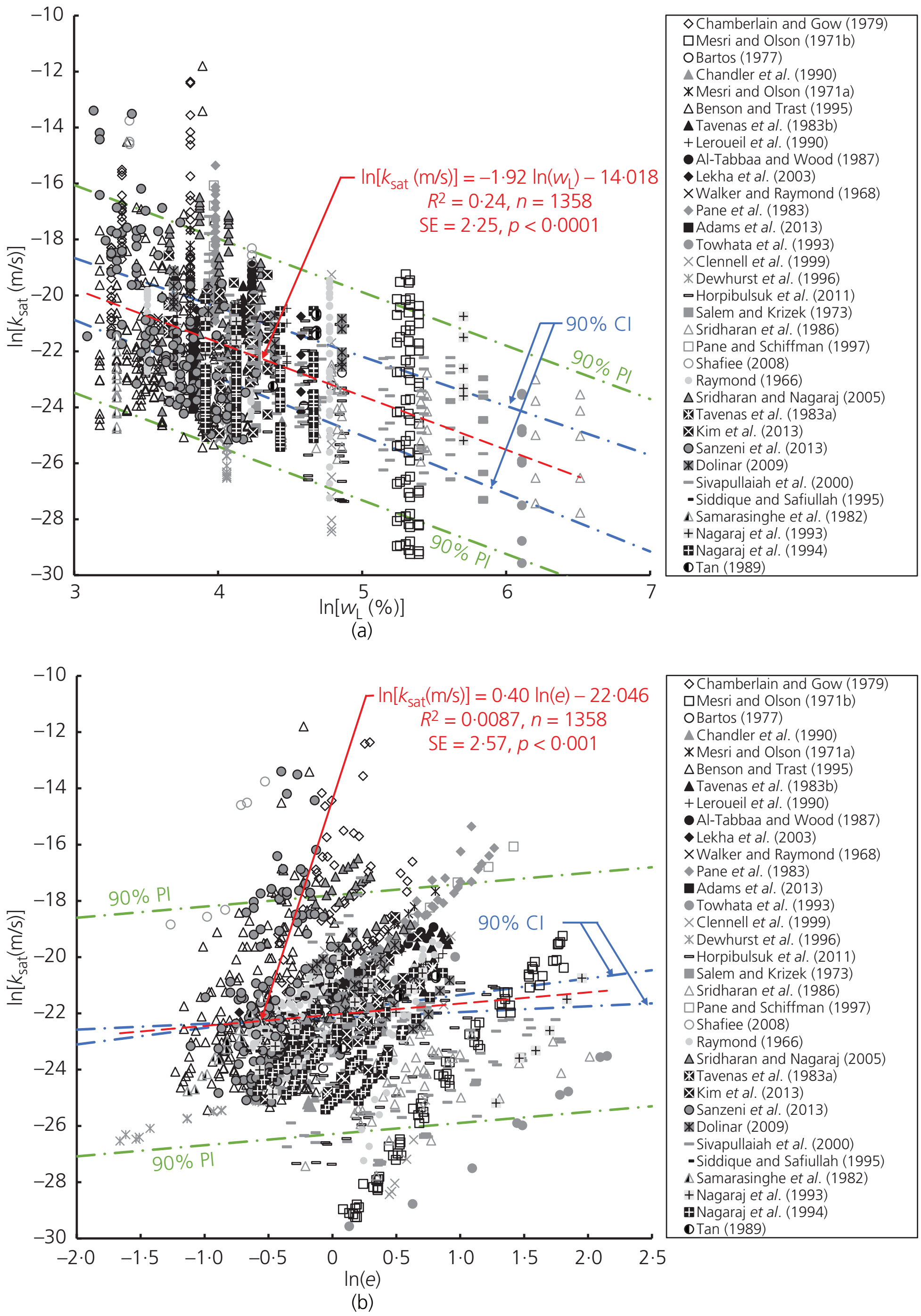

Figure 3. (a) ln k_{sat} plotted against ln w_L; (b) ln k_{sat} plotted against ln e; (c) ln w_L plotted against ln e. CI, confidence interval; PI, prediction interval (continued on next page)

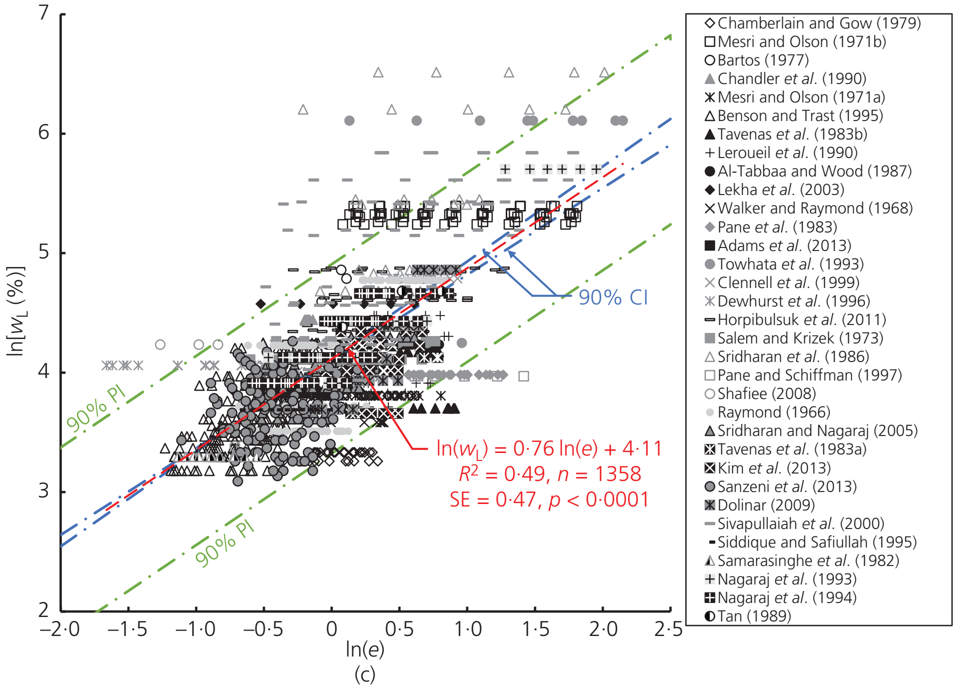

Figure 3. Continued

individual test series and strong correlations for individual soils are present (see Table S1 in the online supplementary material). Table S1 in the online supplementary material shows that for most single soil types, a reliable power correlation exists between k and e. Compared with the regression results between k and $e^3/(1+e)$, the regression results between k and e generally yields a similar R^2 value (average difference in R^2 is 0·001 and 0·24% for RD) for each single soil type. In this paper, e will be used in lieu of $e^3/(1+e)$ for developing the correlation used to predict saturated hydraulic conductivity.

Some covariance between w_L and e in the collected database is observed (see Figure 3(c)). However, the void ratio e and liquidity index w_L can be measured independently of each other, and so regression analyses using both are justified. Figure 4 shows that the 'a' from Equation 7 ($k = ae^b$) is strongly correlated with w_L, thus demonstrating that w_L is an effective normaliser for w. The multiple linear regression of k_{sat} with both e and w_L gives the following equation

$$\ln[k_{sat}(\mathrm{m/s})] = 3{\cdot}78\ln(e) - 4{\cdot}33\ln(w_L) - 4{\cdot}27$$

12a. $$(R^2 = 0{\cdot}64,\ n = 1352,\ \mathrm{SE} = 1{\cdot}54,\ p < 0{\cdot}0001)$$

which can be rearranged to

12b. $$k_{sat}(\mathrm{m/s}) = 0{\cdot}014e^{3{\cdot}78}w_L^{-4{\cdot}33}$$

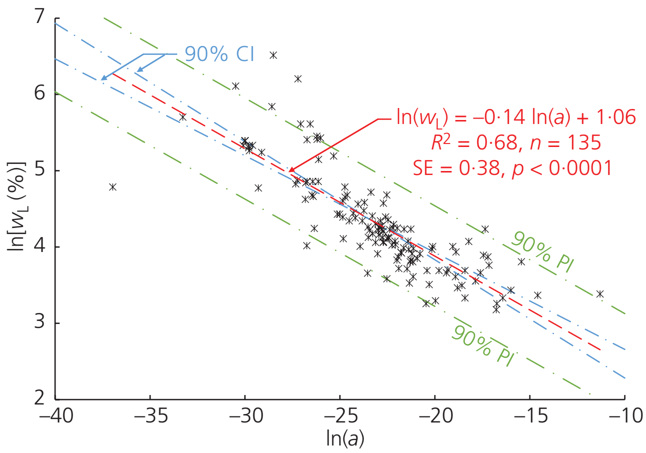

Figure 4. ln w_L plotted against ln a

The six data points from the paper by Shafiee (2008) were excluded from the regression, as examination of these data showed that these were at least two magnitudes higher than those for similar materials of same consolidation states (e.g. Adams *et al.*, 2013; Clennell *et al.*, 1999; Dolinar, 2009; Mesri and Olson, 1971b; Sridharan and Nagaraj, 2005); these data are shown in Figures S1 and S2 in the online supplementary material for reference. Figure 5 presents the k_{sat}-measured against k_{sat}-predicted plot based on Equation 12b, which shows that 10% of the total points fall out of the '$y = 0{\cdot}1x$' and '$y = 10x$' range, 56% of the data points plot below the line of equality (44% above).

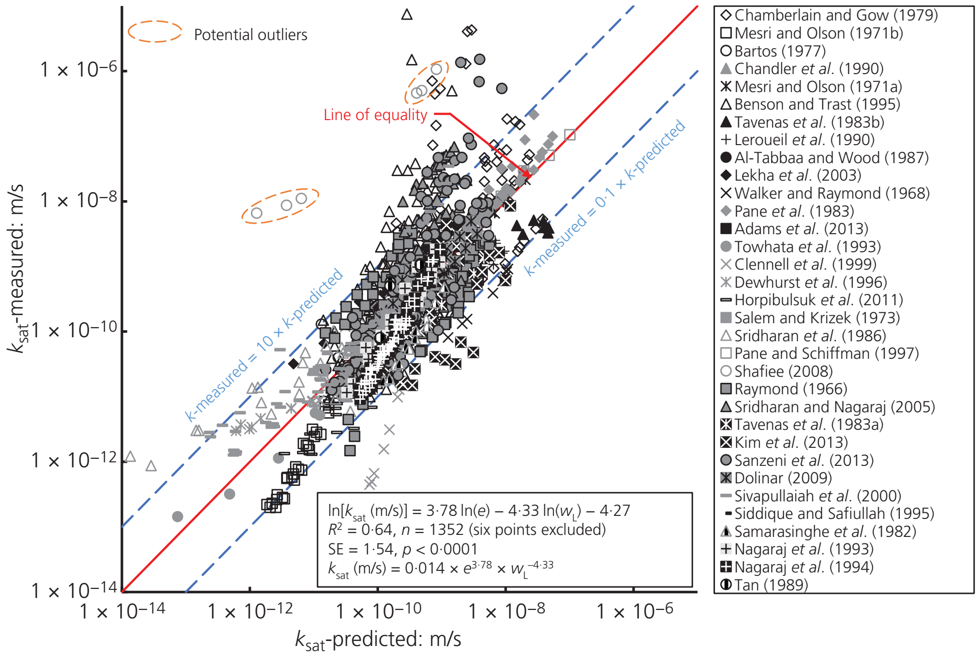

Figure 5. k_{sat}-measured plotted against k_{sat}-predicted (Equation 12)

Equation 12b generally gives a prediction of k_{sat} between 0·1 and 10 times of the measured value and tends to give slightly overpredicted results. However, given that the exponent on e and w_L^{-1} is similar, Equation 12b could be simplified by setting the exponents to equal numerical values

$$\ln[k_{sat}(\mathrm{m/s})] = 4{\cdot}13\ \ln(e/w_L) - 5{\cdot}12$$

13a. $$(R^2 = 0{\cdot}62,\ \ n = 1352,\ \ \mathrm{SE} = 1{\cdot}57,\ \ p < 0{\cdot}0001)$$

which can be rearranged to

13b. $$k_{sat}(\mathrm{m/s}) = 0{\cdot}0060(e/w_L)^{4{\cdot}13}$$

The reported specific gravity (G_S) values in the database range from 2·09 to 2·90. The void ratio e might be further reduced to the saturated water content (w) expressed as a percentage so that $w/w_L(\%) = e/e_L$. Figure 6 shows the correlations between $\ln k_{sat}$ and $\ln(w/w_L)$, which can be rearranged, giving

$$\ln[k_{sat}(\mathrm{m/s})] = 4{\cdot}083\ \ln(w/w_L) - 20{\cdot}074$$

14a. $$(R^2 = 0{\cdot}62,\ \ n = 1352,\ \ \mathrm{SE} = 1{\cdot}58,\ \ p < 0{\cdot}0001)$$

which can be rearranged to

14b. $$k_{sat}(\mathrm{m/s}) = 1{\cdot}91 \times 10^{-9}(w/w_L)^{4{\cdot}083}$$

For the data sources where G_S was not explicitly quoted, the average G_S value of 2·701 (n = 860) based on the entire database was used to calculate w.

Equation 14b uses w/w_L, which is equivalent to the e/e_L ratio given in the papers by Nagaraj *et al*. (1993, 1994) (see Figure 6) and presents a simplified method to make an a priori prediction of k_{sat}. The k_{sat}-measured against k_{sat}-predicted plot (see Figure 7) shows that Equation 14b generally allows for the prediction of k_{sat} between 0·1 and 10 times of the measured value (plus or minus an order of magnitude) (89% of the total points fall within this range) and tends to give slightly overpredicted results (59% plot below the line of equality and 41% above). Equation 14b is compared with the correlations from the papers by Nagaraj *et al*. (1993) (Equation 8), Nagaraj *et al*. (1994) (Equation 9) and Mbonimpa *et al*. (2002) (Equation 10) in Figure 8.

Influence of Atterberg limits

The database is classified into samples with high liquidity ($w_L \geq 50\%$) and low liquidity ($w_L < 50\%$). Figure 9 presents the relationship between $\ln k_{sat}$ and $\ln(w/w_L)$ for each subset. The equations obtained from regression analysis and the corresponding prediction results are summarised in Table 2 (see Figures S3 and S4 in the online supplementary material for the predicted-against-measured plots). The exponent in the regression equation does not vary considerably within different subsets (3·70 against 3·95), with around 90% of the predicted values falling within the $y = 0{\cdot}1x$ and $y = 10x$ bounds. Both subsets generally give a prediction of k_{sat} within 0·1–10 times accuracy. Compared with the low-liquidity subdataset ($w_L < 50\%$), the subdataset with $w_L > 50$ has more reliable (93% within the range) and unbiased

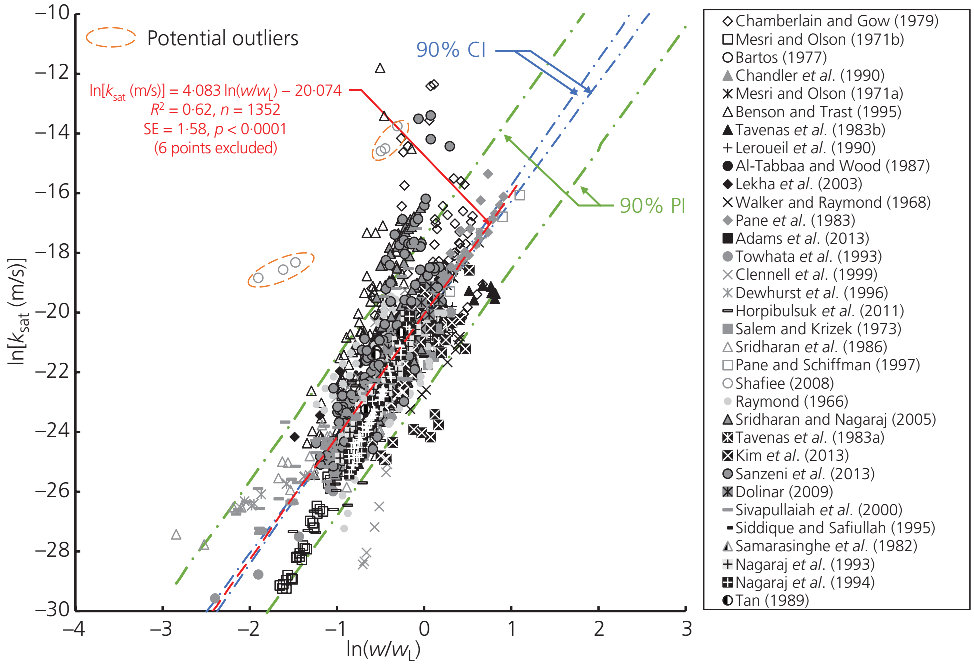

Figure 6. ln k_{sat} plotted against ln(w/w_L)

(52% overpredicted, 48% underpredicted) predictions of k_{sat} with its regressed prediction model.

Figure 10 shows the correlations between ln k_{sat} and ln(w/w_L) for data subsets 'above the A line' (clayey soil) and 'below the A line' (silty soil). For the database presented in this paper, 75 samples did not have I_P or USCS information available and therefore were not included in this part of the analysis. Table 3 summarises the linear regression results and the corresponding prediction outcomes for both data subsets (see Figures S5 and S6 in the online supplementary material for the predicted-against-measured plots). The regression equations of both subdatasets are

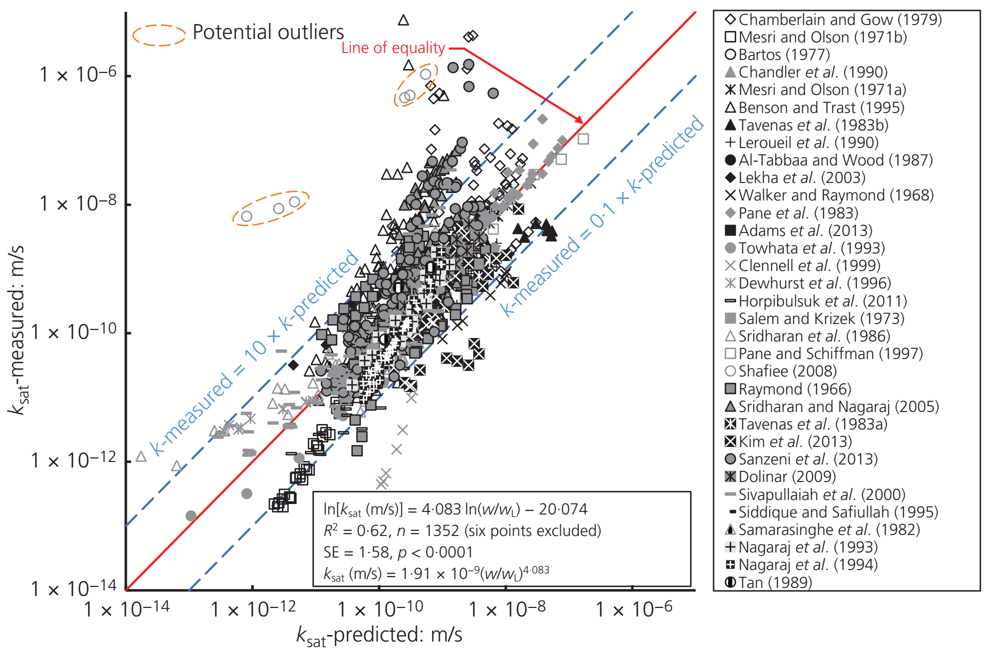

Figure 7. k_{sat}-measured plotted against k_{sat}-predicted (Equation 14)

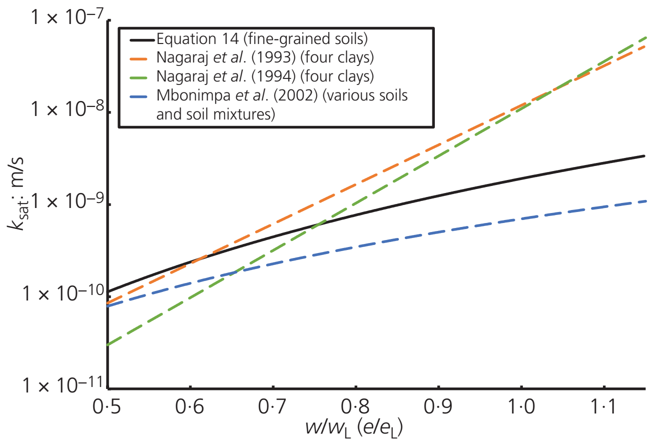

Figure 8. Comparison with previous correlations

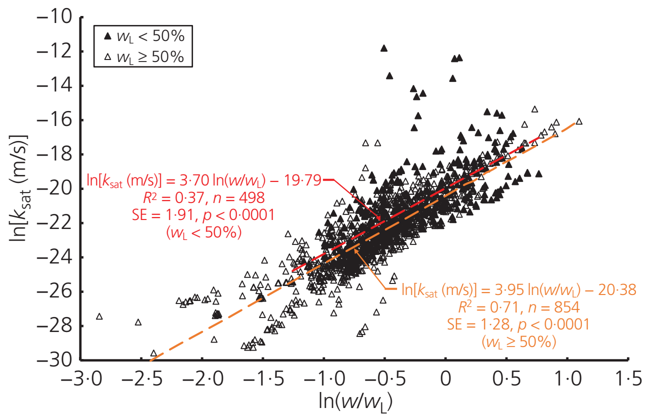

Figure 9. ln k_{sat} plotted against $\ln(w/w_L)$ with soil classified by w_L

similar to the regressed results of the total database (Equation 14b). Both subdatasets provide a prediction of k_{sat} mostly within 0·1–10 times accuracy, while the above the A line (clayey soil) subdataset comes with a higher percentage of data points (89%) falling within the $y = 0{\cdot}1x$ to $y = 10x$ range, while the below the A line (silty soil) subdataset gives a more symmetrical prediction (57% overpredicted; 43% underpredicted) using the regression equation.

Influence of the permeability test method

As listed in Table 1, four different types of hydraulic conductivity measurement approaches are involved in the analysed database. The database is further subdivided based on the reported k test methods to examine the potential effect brought by k test approaches. The ln k_{sat} against $\ln(w/w_L)$ plots of four data subsets are individually presented in Figure 11. Table 4 summarises the analysis results of each data subset (see Figures S7–S10 in the online supplementary material for the measured-against-predicted plots). The exponent in the regressed equation does not fluctuate

Table 2. Analysis results of data subsets classified by w_L level (see also Figures S3 and S4 in the online supplementary material)

Classification	n	Regressed equation	R^2	SE	Between $y = 0{\cdot}1x$ and $y = 10x$: %	Overpredicted: %	Underpredicted: %	Rearranged equation
$w_L < 50$	498	$\ln[k_{sat}(\text{m/s})] = 3{\cdot}70\ln(w/w_L) - 19{\cdot}79$	0·37	1·91	82	62	38	$k_{sat}(\text{m/s}) = 2{\cdot}54 \times 10^{-9}(w/w_L)^{3{\cdot}70}$
$w_L > 50$	854	$\ln[k_{sat}(\text{m/s})] = 3{\cdot}95\ln(w/w_L) - 20{\cdot}38$	0·71	1·28	93	52	48	$k_{sat}(\text{m/s}) = 1{\cdot}41 \times 10^{-9}(w/w_L)^{3{\cdot}95}$
Total	1352							

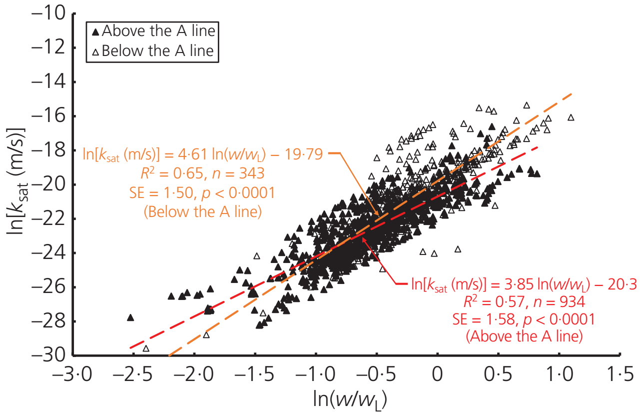

Figure 10. ln k_{sat} plotted against ln(w/w_L) with soil classified by location on the Casagrande chart with respect to the location of the A line

much within different subdatasets, and all four subdatasets provide predictions of k_{sat} mostly within 0·1–10 times of the measured k_{sat}, the 'consolidation test' subdataset has the most data points (93%) fall within the $y = 0{\cdot}1x$ to $y = 10x$ range and also gives the most unbiased prediction results with its regressed equation among the four data subsets.

Influence of test sample states

Finally, the saturated hydraulic conductivity results in the database were subdivided on the basis of samples whose state was able to be classed as 'undisturbed' or 'disturbed' (i.e. those where the natural structure, water content and or stress level were changed during testing from the in situ conditions). The bulk of the database was classified as disturbed, while the test results reported by Walker and Raymond (1968), Tavenas *et al.* (1983a, 1983b), Chandler *et al.* (1990), Leroueil *et al.* (1990) and Kim *et al.* (2013) were identified as undisturbed. Note that the sample states in the paper by Sanzeni *et al.* (2013) (n = 122) were not clearly specified; therefore, these 122 data points were not included in either the disturbed or the undisturbed subset. The correlations between ln k_{sat} and ln(w/w_L) for both the disturbed and undisturbed data subsets are presented in Figure 12. Table 5 shows the regression equation and analyses results for both data subsets (see Figures S11 and S12 in the online supplementary material for the corresponding measured-against-predicted plots). Both subdatasets provide a prediction of k_{sat} mostly within 0·1–10 times accuracy, while the regression equation of the undisturbed data subset gives a better prediction with higher percentage of data points (97%) plotting within the $y = 0{\cdot}1x$ to $y = 10x$ range. The difference in the correlations in these two subsets is more noticeable than in the previous subsets, with the exponent being considerably lower for undisturbed soils.

Concluding remarks

A large database, FG/KSAT-1358 (n > 1300), of saturated hydraulic conductivity measurements on fine-grained materials has been gathered, and a simplified prediction equation was proposed (see

Table 3. Analysis results of data subset classified by location relative to the A line: $I_P = 0{\cdot}73(w_L - 20)$ (see also Figures S5 and S6 in the online supplementary material)

Classification	n	Regressed equation	R^2	SE	Between $y = 0{\cdot}1x$ and $y = 10x$: %	Overpredicted: %	Underpredicted: %	Rearranged equation
Above the A line	934	$\ln k_{sat}(\text{m/s}) = 3{\cdot}85 \ln(w/w_L) - 20{\cdot}30$	0·57	1·58	89	61	39	$k_{sat}(\text{m/s}) = 1{\cdot}53 \times 10^{-9}(w/w_L)^{3{\cdot}85}$
Below the A line	343	$\ln k_{sat}(\text{m/s}) = 4{\cdot}61 \ln(w/w_L) - 19{\cdot}79$	0·65	1·50	87	57	43	$k_{sat}(\text{m/s}) = 2{\cdot}54 \times 10^{-9}(w/w_L)^{4{\cdot}61}$
Total	1277							

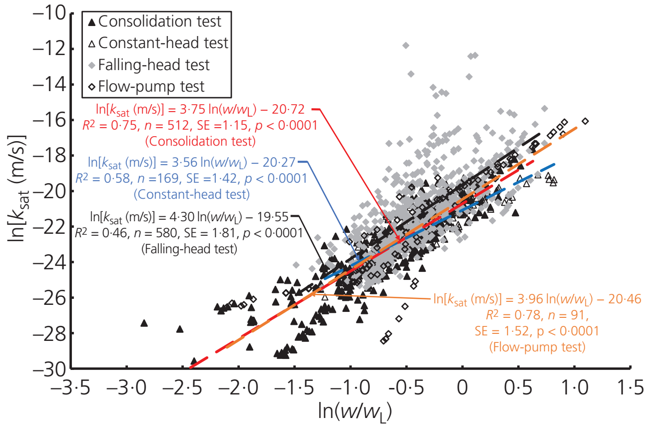

Figure 11. ln k_{sat} plotted against ln(w/w_L) with soil classified by k test methods

Equation 14b). Using the data from the soil database, it is shown that both e and $e^3/(1 + e)$ statistically predict k; the variable in the obtained R^2 is shown to be minor. Use of the water content ratio (w/w_L) is theoretically justified as w is an acceptable surrogate for e and w_L is an acceptable surrogate for S_S, which are two key factors of the Kozeny–Carman equation. This approach has been successfully used by past researchers with smaller datasets.

The prediction equation gives a good prediction of hydraulic conductivity mostly within 0·1–10 times ranges for the whole database. Splitting the database by the w_L level, clay/silts, k test methods and the states of test sample shows minor variation on the regressed equation with the exponent of w/w_L usually around 4. Therefore, Equation 14b offers a theoretically sound, semi-empirical approach to predicting k_{sat} for fine-grained soils.

14b. $$k_{sat}(\mathrm{m/s}) = 1{\cdot}91 \times 10^{-9}(w/w_L)^{4{\cdot}083}$$

The accuracy of Equation 14b could be improved with a database that allows for the correction of all k_{sat} values to a set temperature: some of the scatter in the database is probably due to some variation in the test temperature. While the prediction bounds for Equation 14b are wider than those from the papers of Nagaraj *et al*. (1993, 1994) and Mbonimpa *et al*. (2002), it should be noted that Equation 14 has been calibrated by a much larger database of over 1300 k_{sat} measurements.

Acknowledgements

The first author was supported for this work by a scholarship from the China Scholarship Council (CSC) under CSC Grant Number 201708060067. The authors thank Miss Casey J. Shepheard for her help assembling some of the early entries in the database. The authors also thank Dr Flavia De Luca and Dr Elizabeth Holcombe for their helpful comments and suggestions related to this work. The online supplementary material can be downloaded from the ICE Virtual Library.

Table 4. Analysis results of data subsets classified by k_{sat} test method (see also Figures S7–S10 in the online supplementary material)

Classification	n	Regressed equation	R^2	SE	Between y = 0·1x and y = 10x: %	Overpredicted: %	Underpredicted: %	Rearranged equation
Falling-head	580	$\ln[k_{sat}(\mathrm{m/s})] = 4{\cdot}30 \ln(w/w_L) - 19{\cdot}55$	0·46	1·81	86	59	41	$k_{sat}(\mathrm{m/s}) = 3{\cdot}23 \times 10^{-9}(w/w_L)^{4{\cdot}30}$
Constant-head	169	$\ln[k_{sat}(\mathrm{m/s})] = 3{\cdot}56 \ln(w/w_L) - 20{\cdot}27$	0·58	1·42	90	63	37	$k_{sat}(\mathrm{m/s}) = 1{\cdot}57 \times 10^{-9}(w/w_L)^{3{\cdot}56}$
Consolidation	512	$\ln[k_{sat}(\mathrm{m/s})] = 3{\cdot}75 \ln(w/w_L) - 20{\cdot}72$	0·75	1·15	93	45	55	$k_{sat}(\mathrm{m/s}) = 1{\cdot}00 \times 10^{-9}(w/w_L)^{3{\cdot}75}$
Flow-pump	91	$\ln[k_{sat}(\mathrm{m/s})] = 3{\cdot}96 \ln(w/w_L) - 20{\cdot}46$	0·78	1·52	89	42	58	$k_{sat}(\mathrm{m/s}) = 1{\cdot}30 \times 10^{-9}(w/w_L)^{3{\cdot}96}$
Total	1352							

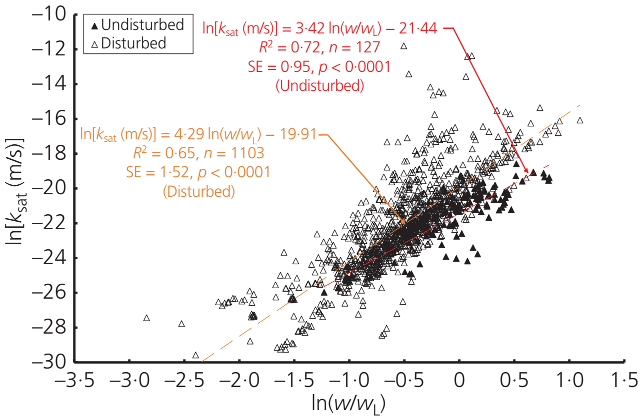

Figure 12. ln k_{sat} plotted against ln(w/w_L) with soil classified by test sample states

Table 5. Analysis results of data subsets classified by states of test samples (see also Figures S11 and S12 in the online supplementary material)

Classification	n	Regressed equation	R^2	SE	Between y = 0·1x and y = 10x: %	Overpredicted: %	Under-predicted: %	Rearranged equation
Disturbed	1103	$\ln[k_{sat}(\text{m/s})] = 4{\cdot}29\ln(w/w_L) - 19{\cdot}91$	0·65	1·52	91	61	39	$k_{sat}(\text{m/s}) = 2{\cdot}26 \times 10^{-9}(w/w_L)^{4{\cdot}29}$
Undisturbed	127	$\ln[k_{sat}(\text{m/s})] = 3{\cdot}42\ln(w/w_L) - 21{\cdot}44$	0·72	0·95	97	48	52	$k_{sat}(\text{m/s}) = 4{\cdot}88 \times 10^{-10}(w/w_L)^{3{\cdot}42}$
Total	1230							

REFERENCES

Adams AL, Germaine JT, Flemings PB and Day-Stirrat RJ (2013) Stress induced permeability anisotropy of Resedimented Boston Blue Clay. *Water Resources Research* **49(10)**: 6561–6571, https://doi.org/10.1002/wrcr.20470.

Al-Moadhen MM, Clarke BG and Chen X (2018) The permeability of composite soils. *Environmental Geotechnics*, https://doi.org/10.1680/jenge.18.00030.

Al-Tabbaa A and Wood DM (1987) Some measurements of the permeability of kaolin. *Géotechnique* **37(4)**: 499–514, https://doi.org/10.1680/geot.1987.37.4.499.

Amadi AA and Alih CO (2019) Hydraulic conductivity of modified clay treated with CKD. *Environmental Geotechnics* **6(1)**: 26–33, https://doi.org/10.1680/jenge.16.00025.

ASTM (2010) D 4318-10: Standard test methods for liquid limit, plastic limit, and plasticity index of soils. ASTM International, West Conshohocken, PA, USA.

ASTM (2017) D 2487-17: Standard practice for classification of soils for engineering purposes (Unified Soil Classification System). ASTM International, West Conshohocken, PA, USA.

Azad S, Farid A and Browning J (2015) Effect of electromagnetic stimulation on hydraulic conductivity. *Environmental Geotechnics* **2(4)**: 211–223, https://doi.org/10.1680/envgeo.13.00027.

Bannour H, Goblet P, Mendes M and Touze-Foltz N (2016) Numerical study of advective flow through composite liners. *Environmental Geotechnics* **3(6)**: 379–385, https://doi.org/10.1680/envgeo.14.00043.

Bartos MJ (1977) *Classification and Engineering Properties of Dredged Material*. Environmental Effects Laboratory, US Army Engineer Waterways Experiment Station, Vicksburg, MS, USA. Technical Report D-77-18.

Benson CH and Trast JM (1995) Hydraulic conductivity of thirteen compacted clays. *Clays and Clay Minerals* **43(6)**: 669–681, https://doi.org/10.1346/CCMN.1995.0430603.

BSI (1975) BS 1377:1975: Methods of test for soils for civil engineering purposes. BSI, London, UK.

BSI (1990) BS 1377:1990: Methods of test for soils for civil engineering purposes. BSI, London, UK.

Carman PC (1937) Fluid flow through granular beds. *Transactions of the Institution of Chemical Engineers* **15**: 150–166, https://doi.org/10.1016/S0263-8762(97)80003-2.

Carman PC (1939) Permeability of saturated sands, soils and clays. *Journal of Agricultural Science* **29(2)**: 262–273, https://doi.org/10.1017/S0021859600051789.

Carrier WD and Beckman JF (1984) Correlations between index tests and the properties of remoulded clays. *Géotechnique* **34(2)**: 211–228, https://doi.org/10.1680/geot.1984.34.2.211.

Chamberlain EJ and Gow AJ (1979) Effect of freezing and thawing on the permeability and structure of soils. *Developments in Geotechnical Engineering* **26(C)**: 73–92, https://doi.org/10.1016/B978-0-444-41782-4.50012-9.

Chandler RJ, Leroueil S and Trenter NA (1990) Measurements of the permeability of London Clay using a self-boring permeameter. *Géotechnique* **40(1)**: 113–124, https://doi.org/10.1680/geot.1990.40.1.113.

Chapuis RP (2012) Predicting the saturated hydraulic conductivity of soils: a review. *Bulletin of Engineering Geology and the Environment* **71(3)**: 401–434, https://doi.org/10.1007/s10064-012-0418-7.

Chapuis RP and Aubertin M (2003) On the use of the Kozeny–Carman equation to predict the hydraulic conductivity of soils. *Canadian Geotechnical Journal* **40(3)**: 616–628, https://doi.org/10.1139/t03-013.

Ching J, Arroyo M, Chen J *et al.* (2017) Transformation models and multivariate soil databases. In *Joint TC205/TC304 Working Group on 'Discussion of Statistical/Reliability Methods for Eurocodes'* (ISSMGE (International Society for Soil Mechanics and Geotechnical Engineering) (ed.)). ISSMGE, London, UK, pp. 1–19.

Chung SG, Giao PH, Kim GJ and Leroueil S (2002) Geotechnical properties of Pusan clays. *Canadian Geotechnical Journal* **39(5)**: 1050–1060, https://doi.org/10.1139/t02-055.

Clennell MB, Dewhurst DN, Brown KM and Westbrook GK (1999) Permeability anisotropy of consolidated clays. In *Muds and Mudstones: Physical and Fluid Flow Properties* (Aplin AC, Fleet AJ and MacQuaker JHS (eds)). Geological Society of London, London, UK, vol. 158, pp. 79–96.

De Bruyn CMA, Collins LE and Williams AAB (1957) The specific surface, water affinity, and potential expansiveness of clays. *Clay Minerals* **3(17)**: 120–128, https://doi.org/10.1180/claymin.1957.003.17.02.

Dewhurst DN, Brown KM, Clennell MB and Westbrook GK (1996) A comparison of the fabric and permeability anisotropy of consolidated and sheared silty clay. *Engineering Geology* **42(4)**: 253–267, https://doi.org/10.1016/0013-7952(95)00089-5.

Dolinar B (2009) Predicting the hydraulic conductivity of saturated clays using plasticity–value correlations. *Applied Clay Science* **45(1–2)**: 90–94, https://doi.org/10.1016/j.clay.2009.04.001.

Dong S, Guo Y and Yu X (2018) Procedures for quick estimation of hydraulic conductivity of unsaturated soils. *Environmental Geotechnics*, https://doi.org/10.1680/jenge.17.00070.

Farrar DM and Coleman JD (1967) The correlation of surface area with other properties of nineteen British clay soils. *Journal of Soil Science* **18(1)**: 118–124, https://doi.org/10.1111/j.1365-2389.1967.tb01493.x.

Griffiths FJ and Joshi RC (1988) Identification of cementation in overconsolidated clays. *Géotechnique* **38(3)**: 451–452, https://doi.org/10.1680/geot.1988.38.3.451.

Hamm NAS, Hall JW and Anderson MG (2006) Variance-based sensitivity analysis of the probability of hydrologically induced slope stability. *Computers and Geosciences* **32(6)**: 803–817, https://doi.org/10.1016/j.cageo.2005.10.007.

Hobbs P, Jones L, Kirkham M, Gunn D and Entwisle D (2018) Shrinkage limit test results and interpretation for clay soils. *Quarterly Journal of Engineering Geology and Hydrology* **52(2)**: 220–229, https://doi.org/10.1144/qjegh2018-100.

Horpibulsuk S, Yangsukkaseam N, Chinkulkijniwat A and Du YJ (2011) Compressibility and permeability of Bangkok clay compared with kaolinite and bentonite. *Applied Clay Science* **52(1–2)**: 150–159, https://doi.org/10.1016/j.clay.2011.02.014.

Kim HS, Cho GC, Lee JY and Kim SJ (2013) Geotechnical and geophysical properties of deep marine fine-grained sediments recovered during the second Ulleung Basin Gas Hydrate expedition, East Sea, Korea. *Marine and Petroleum Geology* **47**: 56–65, https://doi.org/10.1016/j.marpetgeo.2013.05.009.

Kozeny J (1927) Über kapillare Leitung des Wassers im Boden (Aufstieg, Versickerung und Anwendung auf die Bewässerung). *Sitzungsberichte der Kaiserlichen Akademie der Wissenschaften in Wien* **136a**: 271–306 (in German).

Kulhawy FH and Mayne PW (1990) *Manual on Estimating Soil Properties for Foundation Design*. Electric Power Research Institute, Palo Alto, CA, USA, Report. No. EL-6800.

Kuriakose B, Abraham BM, Sridharan A and Jose BT (2017) Water content ratio: an effective substitute for liquidity index for prediction of shear strength of clays. *Geotechnical and Geological Engineering* **35(4)**: 1577–1586, https://doi.org/10.1007/s10706-017-0193-0.

Lekha KR, Krishnaswamy NR and Basak P (2003) Consolidation of clays for variable permeability and compressibility. *Journal of Geotechnical and Geoenvironmental Engineering* **129(11)**: 1001–1009, https://doi.org/10.1061/%28ASCE%291090-0241%282003%29129%3A11%281001%29.

Leroueil S, Bouclin G, Tavenas F, Bergeron L and La Rochelle P (1990) Permeability anisotropy of natural clays as a function of strain. *Canadian Geotechnical Journal* **27(5)**: 568–579, https://doi.org/10.1139/t90-072.

Locat J, Lefebvre G and Ballivy G (1984) Mineralogy, chemistry, and physical properties interrelationships of some sensitive clays from Eastern Canada. *Canadian Geotechnical Journal* **21(3)**: 530–540, https://doi.org/10.1139/t84-055.

Mbonimpa M, Aubertin M, Chapuis R and Busssière B (2002) Practical pedotransfer functions for estimating the saturated hydraulic conductivity. *Geotechnical and Geological Engineering* **20(3)**: 235–259, https://doi.org/10.1023/A:1016046214724.

Mesri G and Olson RE (1971a) Mechanisms controlling the permeability of clays. *Clays and Clay Minerals* **19(3)**: 151–158, https://doi.org/10.1346/CCMN.1971.0190303.

Mesri G and Olson RE (1971b) Consolidation characteristics of montmorillonite. *Géotechnique* **21(4)**: 341–352, https://doi.org/10.1680/geot.1971.21.4.341.

Montgomery DC, Runger GC and Hubele NF (2007) *Engineering Statistics*, 4th edn. Wiley New York, NY, USA.

Mualem Y (1976) A new model for predicting the hydraulic conductivity of unsaturated porous media. *Water Resources Research* **12(6)**: 1248–1254, http://doi.org/10.1029/WR012i003p00513.

Muhunthan B (1991) Liquid limit and surface area of clays. *Géotechnique* **41(1)**: 135–138, https://doi.org/10.1680/geot.1991.41.1.135.

Nagaraj TS and Srinivasa Murthy BR (1986) A critical reappraisal of compression index equations. *Géotechnique* **36(1)**: 27–32, https://doi.org/10.1680/geot.1986.36.1.27.

Nagaraj TS, Pandian NS and Narashimha Raju PSR (1993) Stress state–permeability relationships for fine-grained soils. *Géotechnique* **43(2)**: 333–336, https://doi.org/10.1680/geot.1993.43.2.333.

Nagaraj TS, Pandian NS and Narashimha Raju PSR (1994) Stress state–permeability relations for overconsolidated clays. *Géotechnique* **44(2)**: 349–352, https://doi.org/10.1680/geot.1994.44.2.349.

O'Kelly BC (2016) Briefing: Laboratory permeability determination for biosolids. *Environmental Geotechnics* **3(3)**: 132–139, https://doi.org/10.1680/jenge.15.00026.

O'Kelly BC, Vardanega PJ and Haigh SK (2018) Use of fall cones to determine Atterberg limits: a review. *Géotechnique* **68(10)**: 843–856, https://doi.org/10.1680/jgeot.17.R.039, plus corrigendum, **68(10)**: 935.

Olson R and Daniel D (1981) Measurement of the hydraulic conductivity of fine-grained soils. In *Permeability and Groundwater Contaminant Transport* (Zimmie T and Riggs C (eds)). ASTM International, West Conshohocken, PA, USA, STP746-EB, pp. 18–64.

Pane V and Schiffman RL (1997) The permeability of clay suspensions. *Géotechnique* **47(2)**: 273–288, https://doi.org/10.1680/geot.1997.47.2.273.

Pane V, Croce P, Znidarcic D *et al.* (1983) Effects of consolidation on permeability measurements for soft clay. *Géotechnique* **33(1)**: 67–72, https://doi.org/10.1680/geot.1983.33.1.67.
Phoon KK and Kulhawy FH (1999a) Characterization of geotechnical variability. *Canadian Geotechnical Journal* **36(4)**: 612–624, https://doi.org/10.1139/t99-038.
Phoon KK and Kulhawy FH (1999b) Evaluation of geotechnical property variability. *Canadian Geotechnical Journal* **36(4)**: 625–639, https://doi.org/10.1139/t99-039.
Raymond GP (1966) Laboratory consolidation of some normally consolidated soils. *Canadian Geotechnical Journal* **3(4)**: 217–234, https://doi.org/10.1139/t66-026.
Ren XW and Santamarina JC (2018) The hydraulic conductivity of sediments: a pore size perspective. *Engineering Geology* **233**: 48–54, https://doi.org/10.1016/j.enggeo.2017.11.022.
Ren X, Zhao Y, Deng Q *et al.* (2016) A relation of hydraulic conductivity–void ratio for soils based on Kozeny–Carman equation. *Engineering Geology* **213**: 89–97, https://doi.org/10.1016/j.enggeo.2016.08.017.
Salem AM and Krizek RJ (1973) Consolidation characteristics of dredging slurries. *Journal of the Waterways Harbors and Coastal Engineering Division* **99(4)**: 439–457.
Samarasinghe AM, Huang YH and Drnevich VP (1982) Permeability and consolidation of normally consolidated soils. *Journal of the Geotechnical Engineering Division* **108(6)**: 835–850.
Santoso AM, Phoon KK and Quek ST (2011) Probability models of SWCC and hydraulic conductivity. *Proceedings of the 14th Asian Regional Conference on Soil Mechanics and Geotechnical Engineering 2011: Challenges and Solutions, Hong Kong, China*, vol. 3, pp. 2377–2381.
Sanzeni A, Colleselli F and Grazioli D (2013) Specific surface and hydraulic conductivity of fine-grained soils. *Journal of Geotechnical and Geoenvironmental Engineering* **139(10)**: 1828–1832, https://doi.org/10.1061/(ASCE)GT.1943-5606.0000892.
Shafiee A (2008) Permeability of compacted granule-clay mixtures. *Engineering Geology* **97(3–4)**: 199–208, https://doi.org/10.1016/j.enggeo.2008.01.002.
Siddique A and Safiullah AMM (1995) Permeability characteristics of reconstituted Dhaka clay. *Journal of the Civil Engineering Division* **23(1)**: 103–115.
Sivapullaiah PV, Sridharan A and Stalin VK (2000) Hydraulic conductivity of bentonite–sand mixtures. *Canadian Geotechnical Journal* **37(2)**: 406–413, https://doi.org/10.1139/t99-120.
Spagnoli G and Feinendegen M (2017) Relationship between measured plastic limit and plastic limit estimated from undrained shear strength, water content ratio and liquidity index. *Clay Minerals* **52(4)**: 509–519, https://doi.org/10.1180/claymin.2017.052.4.08.
Sridharan A and Nagaraj HB (2005) Hydraulic conductivity of remolded fine-grained soils versus index properties. *Geotechnical and Geological Engineering* **23(1)**: 43–60, https://doi.org/10.1007/s10706-003-5396-x.
Sridharan A and Choudhary D (2008) Computation of hydraulic conductivity of montmorillonitic clays by diffuse double layer theory. *International Journal of Geotechnical Engineering* **2(1)**: 1–10, https://doi.org/10.3328/IJGE.2008.02.01.1-10.
Sridharan A, Rao S and Murthy N (1986a) Liquid limit of montmorillonite soils. *Geotechnical Testing Journal* **9(3)**: 156–159, https://doi.org/10.1520/GTJ10623J.
Sridharan A, Rao SM and Murthy NS (1986b) Compressibility behaviour of homoionized bentonites. *Géotechnique* **36(4)**: 551–564, https://doi.org/10.1680/geot.1986.36.4.551.
Sridharan A, Rao SM and Murthy NS (1988) Liquid limit of kaolinitic soils. *Géotechnique* **38(2)**: 191–198, https://doi.org/10.1680/geot.1988.38.2.191.
Tan SA (1989) A simple automatic falling-head permeameter. *Soils and Foundations* **29(1)**: 161–164, https://doi.org/10.3208/sandf1972.29.161.
Tavenas F, Leblond P, Jean P and Leroueil S (1983a) The permeability of natural soft clays – part I: methods of laboratory measurement. *Canadian Geotechnical Journal* **20(4)**: 629–644, https://doi.org/10.1139/t83-072.
Tavenas F, Jean P, Leblond P and Leroueil S (1983b) The permeability of natural soft clays – part II: permeability characteristics. *Canadian Geotechnical Journal* **20(4)**: 645–660, https://doi.org/10.1139/t83-073.
Terzaghi K, Peck RB and Mesri G (1996) *Soil Mechanics in Engineering Practice*, 3rd edn. Wiley, New York, NY, USA.
Towhata I, Kuntiwattanaku P, Seko I and Ohishi K (1993) Volume change of clays induced by heating as observed in consolidation tests. *Soils and Foundations* **33(4)**: 170–183, https://doi.org/10.3208/sandf1972.33.4_170.
Vardanega PJ, Feng S and Shepheard CJ (2017) Some recent research on the hydraulic conductivity of road materials. In *Bearing Capacity of Roads, Railways and Airfields: Proceedings of the 10th International Conference on the Bearing Capacity of Roads, Railways and Airfields (BCRRA 2017), June 28–30, 2017, Athens, Greece* (Loizos A, Al-Qadi I and Scarpas T (eds)). CRC Press/Balkema, Leiden, the Netherlands, pp. 135–142.
Walker LK and Raymond GP (1968) The prediction of consolidation rate in a cemented clay. *Canadian Geotechnical Journal* **5(4)**: 192–216, https://doi.org/10.1139/t68-022.
Waters TJ and Vardanega PJ (2009) Re-examination of the coefficient of determination (r^2) using road materials engineering case studies. *Road and Transport Research* **18(3)**: 3–12.

How can you contribute?

To discuss this paper, please submit up to 500 words to the editor at journals@ice.org.uk. Your contribution will be forwarded to the author(s) for a reply and, if considered appropriate by the editorial board, it will be published as a discussion in a future issue of the journal.